

The 2-dimensional non-linear σ -model on a random lattice

B. Allés and M. Beccaria

Dipartimento di Fisica dell'Università and INFN

Piazza Torricelli 2, I-56100 Pisa, Italy

Abstract

The $O(n)$ non-linear σ -model is simulated on 2-dimensional regular and random lattices. We use two different levels of randomness in the construction of the random lattices and give a detailed explanation of the geometry of such lattices. In the simulations, we calculate the mass gap for $n = 3, 4$ and 8, analysing the asymptotic scaling of the data and computing the ratio of Lambda parameters $\Lambda_{\text{random}}/\Lambda_{\text{regular}}$. These ratios are in agreement with previous semi-analytical calculations. We also numerically calculate the topological susceptibility by using the cooling method.

PACS number(s):05.50.+q 11.15.Ha

arXiv:hep-lat/9503025v2 28 Mar 1995

I. INTRODUCTION

Numerical simulations of an asymptotically free field theory on a lattice provide information about continuum physics when they are performed at values of the correlation length which lay within the scaling window. This region is defined by the inequalities $1 \ll \xi/a \ll L$ where a , ξ and L are the lattice spacing, the correlation length and the lattice size respectively.

To this window it corresponds another scaling window in terms of the bare coupling g . To understand the relationship between both regions, it is enough to recall that $\xi/a \propto \Lambda \exp(1/\alpha)$ where α is proportional to some power of g . In this expression, Λ is the renormalization group independent mass parameter. This parameter depends on the regularization used, thus the scaling window in terms of the bare coupling can be shifted towards the region of lower couplings if we use a lattice regularization in which Λ is small. Gauge theories regularized on a random lattice present a Λ parameter some orders of magnitude smaller than on a regular square lattice [1]. Therefore, the simulations on a random lattice can be performed at lower values of the bare coupling.

This fact may make the simulations on random lattices more advantageous than on regular square lattices. The physical signal in the Monte Carlo data can be masked by the presence of perturbative expansions related to mixings, perturbative tails and finite renormalizations of composite operators defined on the lattice. If the expansion parameter is smaller (and the perturbative coefficients do not get larger), these perturbative terms may be better controlled and the non-perturbative physical signal be more clearly seen. Also the non-universal terms in the scaling function could be less relevant, thus expediting the asymptotic scaling.

The computation of the perturbative coefficients on random lattices might seem rather involved. However, the higher degree of rotational invariance on a random lattice should help in this respect [2].

In order to address these prospects on a physically interesting theory, like QCD, in reference [3] one of us started to study some features concerning another asymptotically free field theory, the $O(n)$ non-linear σ -model in two dimensions. The action for this model in the continuum is

$$\mathcal{S} = \frac{1}{2g} \int d^2x (\partial_\mu \vec{\phi}(x))^2, \quad (1.1)$$

with the constraint $\vec{\phi}(x)^2 = 1$ for all x . In reference [3] we chose this theory because of its properties in common with QCD. Indeed, it is an asymptotically free field theory [4] and presents a topological content [5] for $n = 3$. Moreover, its mass gap is exactly known [6]. It was shown that the first coefficients of the renormalization group functions $\beta(g)$ and $\gamma(g)$ for

this model regularized on a random lattice are universal and that the Λ parameter depends on the degree of randomness κ (see below) used in the construction of the random lattice.

The present work has several aims. Firstly, we want to verify the κ dependence of the Λ parameter and support the scenario of a common continuum limit, the same than that of the theory defined in Eq. (1.1). For this purpose, the theory with $n = 3, 4$ and 8 has been simulated on both regular and random lattices to extract the topological susceptibility and mass gap. We have also successfully used the cooling method [7,8] on a random lattice to extract the topological content of the theory. The $n = 3$ value was chosen to study both the topological susceptibility and the mass gap, while the higher values of n were used in order to have a better asymptotic scaling [9] on the mass gap data. Another reason to study the topological charge on random lattices is that some sites on these lattices can group together forming clusters with a typical size less than one lattice spacing. This geometry might allow the existence of very small instantons which could hardly survive on regular lattices. We have always used lattices large compared to the correlation length at our β , with $L = 200, 300$ and 400 . We have never averaged the results of the simulations among different random lattices because the previous lattice sizes are large enough to include an implicit average among several subregions of the lattice. The updating has been performed by using a cluster algorithm [10] adapted to the random lattice.

Another purpose of the present work is to analyse whether the simulations on a random lattice improve the asymptotic scaling or not. Actually, this is easy to check with the mass gap data because the value of m/Λ is known [6]. As it was shown in [3], $\Lambda_{\text{random}} \approx \Lambda_{\text{regular}}$ for the σ -model. Hence, it is not expected any dramatic shift of the scaling window towards small values of the bare coupling.

To construct the random lattice, we followed the procedure of T. D. Lee et al. [11]. The only new ingredient is the introduction of a degree of randomness κ . The sites of the lattice are the centers of hard spheres, the radius of which is $a/2\kappa$. These hard spheres are randomly located. At small values of κ , the lattice is locally less random as we will see in section 2. There is a κ_{min} at which all distributions (link lengths, distance between neighbouring sites, plaquette areas, etc.) become Dirac deltas.

The plan of the paper is as follows. In section 2, we explain how to construct a random lattice and discuss in detail both the κ dependence and some geometrical properties like average link lengths and average distance between neighbouring sites. We also give a geometrical argument in favour of a unique random lattice, once κ is fixed, as the number of sites gets larger. In section 3 we explain the simulation algorithm used. In section 4 we recall the scaling and β functions for the non-linear σ model. We also explain the procedure followed to extract both the mass gap and the topological susceptibility. A detailed description of the cooling method is also given. In section 5 we show and analyse the Monte Carlo data for the physical observables described in section 4. The conclusions are presented in

section 6.

II. CONSTRUCTION AND GEOMETRY OF A RANDOM LATTICE

We define a random lattice as a set of N points located at random on a volume V with the condition that there are no two sites closer than a/κ where a is the lattice spacing and κ is a parameter to be fixed. These sites are placed with periodic boundary conditions. Thus, we consider the 2-dimensional lattice as a torus. In order to simulate a field theory on this geometry, we must define a net of connections throughout the lattice, linking neighbouring sites. In the first part of the section, we will explain how to place the sites on the lattice and in the second part we will review the triangularization process which is used to construct the links and plaquettes. Finally, we will give some properties of the random lattices.

If N sites are placed on a 2-dimensional volume V , we define the lattice spacing a as $a = \sqrt{V/N}$. The sites of our random lattice are the centers of hard spheres (actually discs), the radii of which are $a/2\kappa$. Thus, the sites are not closer than a/κ . Fixing the parameter $\kappa \in [\kappa_{\min}, \infty]$ yields random lattices of different degrees of randomness as we will see. The value of κ_{\min} can be determined with the following argument. For large values of κ , the discs are small and they can be placed loosely on the volume V . Then, the distributions of link lengths, distances between sites, etc. display a wide dispersion of values. Instead, for small κ there is less play in placing the discs and consequently the distributions show a smaller variance. On a regular square lattice, the hard discs will be placed as in Figure 1a. In this case, $\kappa = 1$. But also when $\kappa = 1$ there can be a bit of dispersion in the distributions characterizing the geometry of the lattice. For example, if we shift one column as shown in Figure 1b ¹ then the distance r_i from any site i to its closest neighbour still satisfies $r_i \geq a$. However, the link lengths are no longer all equal to a . In particular, the links joining the shifted sites with their non-shifted neighbours are strictly longer than a . Thus, a lattice constructed with $\kappa = 1$ need not be regular. The usual regular square lattice is only a particular case of the lattice with $\kappa = 1$.

From these considerations, one can conclude that the smallest κ is reached when the hard discs are packed tight as in Figure 2, forming an hexagonal lattice. In this case, the hard nature of the discs prevent the sites from shifting or moving from their positions in the Figure. Therefore, all link lengths, distances between sites, etc. are the same. Stated in other words, the corresponding distributions are Dirac deltas. As a consequence, the corresponding

¹Due to the periodic boundary conditions we imposed, the piece of disc which exceeds the allowed volume from below, will reappear on the top of the lattice.

κ must be the smallest allowed. The volume occupied by a regular hexagonal lattice with $N = L^2$ sites is $V = L^2\sqrt{3}/2$, hence the parameter κ is $\kappa_{\min} = \sqrt{\sqrt{3}/2} \approx 0.9306049$.

An explicit recipe for putting the N sites on the volume of the lattice is the following. The first site must be put at random in any position on the volume V . Now, imagine we have already placed $\nu < N$ sites, then, by using the random generator, we propose the coordinates of the $(\nu + 1)$ -th site and check that its distance to all the ν previously accepted sites is less than a/κ . If the check is satisfied, we accept this site. If not, we reject it and repeat the process by proposing another $(\nu + 1)$ -th site.

This procedure is repeated until all N sites have been placed on the lattice. Clearly, the number of proposed sites N_p satisfies $N_p \geq N$. In Figure 3 we plot the experimental ratio N_p/N as a function of κ obtained during the construction of lattices with 100 and 1000 sites. From this plot, it is clear that the construction of random lattices with small κ is quite time consuming. One can speed up the check about distances by dividing the volume V into boxes, large enough to contain a few sites on average. Then, the check for a proposed site is performed in the box it belongs to and in its neighbouring boxes. However, even with this improvement, creating lattices with $\kappa < 1.2$ is almost impossible with our recipe. The smallest value of κ we have used in our simulations is $\kappa = 1.3$.

The ratio N_p/N depends only on κ , not on N . Figure 3 confirms this statement. Let us derive a theoretical expression for the curve in Figure 3 for large κ . If a site cannot have neighbours closer than a distance a/κ , then once ν sites have already been placed, the area left free for putting new sites is $V - \nu\pi(a/\kappa)^2$. This expression does not take into account the fact that these circles of radius a/κ can overlap (with the constraint of leaving their centers, the sites, not covered). For large κ , the overlaps are less frequent and the previous formula is adequate. Therefore, the probability for a proposed point to be accepted after having put ν sites is

$$p_\nu = 1 - \frac{\nu\pi a^2}{V\kappa^2}. \quad (2.1)$$

Now, using $a^2 = V/N$, we conclude that the total number of proposed sites divided by N is

$$\frac{1}{N} \sum_{\nu=1}^N \frac{1}{1 - \frac{\nu\pi}{N\kappa^2}}. \quad (2.2)$$

For large enough N , the sum becomes an integral giving the ratio N_p/N as a function of κ

$$N_p/N \approx \int_0^1 \frac{dx}{1 - \frac{x\pi}{\kappa^2}} = -\frac{\ln(1 - \pi/\kappa^2)}{\pi/\kappa^2}. \quad (2.3)$$

This expression, as previously stated, is independent of N . It works well for $\kappa > 2.5$.

Once the lattice volume V has been filled with the N sites for some chosen value of κ , we proceed to the triangularization process. We follow the method of reference [12]. It

consists in joining sets of three sites to form a triangle with the only condition that the circle circumscribed by these three points does not contain any other site. The sides of that triangle are the links joining the three sites and the triangle itself is a plaquette. This construction is unique and fills the whole lattice with no overlapping among the triangles [11]. We also impose periodic boundary conditions in the triangularization process. In Figure 4 we show two $N = 100$ sites random lattices, with $\kappa = \infty$ and $\kappa = 1.3$.

It is useful to define also the dual lattice. Its dual sites are the centers of the above-mentioned circumscribed circles. It is clear that any link is the common side of two triangles. Thus, every link of the random lattice must be surrounded by two dual sites. The line joining these two dual sites is called the dual link. Therefore, every link is associated with a dual link.

Let us call l_{ij}^μ the μ -component of the link vector that points from the site i to the site j . The length of this link is $l_{ij} = \|\mathbf{l}_{ij}\|$. The length of the corresponding dual link is s_{ij} . Throughout this work, we will often make use of the matrix λ_{ij} defined as

$$\lambda_{ij} \equiv \begin{cases} s_{ij}/l_{ij}, & \text{if } i \text{ and } j \text{ are linked;} \\ 0, & \text{otherwise.} \end{cases} \quad (2.4)$$

We introduce another vector, \mathbf{d}_{ij} which is twice the vector joining the center of the vector link \mathbf{l}_{ij} with the center of the associated dual link \mathbf{s}_{ij} . Another useful quantity is σ_{ijk} defined as

$$\sigma_{ijk} \equiv [(\mathbf{l}_{ij} + \mathbf{d}_{ij}) \times (\mathbf{l}_{ik} + \mathbf{d}_{ik})] \cdot \hat{\mathbf{z}}. \quad (2.5)$$

In this equation $\hat{\mathbf{z}}$ is the unit vector orthonormal to the plane of the lattice, oriented as $\hat{\mathbf{z}} = \hat{\mathbf{x}} \times \hat{\mathbf{y}}$.

The set of dual links around the site i , $\{\mathbf{s}_{ij}\}_{i \text{ fixed}}$, determine a convex region called Voronoi cell. The area of this cell is ω_i .

As soon as the lattice has been constructed, one can devise tests to check the triangularization. The first and easiest one is to verify that the number of triangles (links) is equal to twice (three times) the number of sites [11]. Other good tests are the integral properties [13]

$$\sum_j \lambda_{ij} l_{ij}^\mu = 0, \quad \sum_j \lambda_{ij} l_{ij}^\mu (l_{ij}^\nu + d_{ij}^\nu) = 2\omega_i \delta^{\mu\nu}. \quad (2.6)$$

A third test consists in demanding that the quadratic part of the action has only one zero mode [3].

The action for the 2-dimensional $O(n)$ non-linear σ -model on a random lattice can be written as [13]

$$\mathcal{S}^L = \frac{1}{4g} \sum_{i,j} \lambda_{ij} (\vec{\phi}_i - \vec{\phi}_j)^2. \quad (2.7)$$

In this equation, g is the coupling constant. i, j, \dots denote sites and $\vec{\phi}_i$ stands for the value of the field $\vec{\phi}$ at the site i . This is the action we will make use in our numerical simulations, both on regular and random lattices. For a regular square lattice, λ_{ij} is 1 for linked sites and zero otherwise. Hence, Eq. (2.7) becomes the standard action when it is considered on a regular lattice. One can show that the *naïve* continuum limit of Eq. (2.7) is the correct action for the model in the continuum, Eq. (1.1).

We see from Figure 4 that random lattices with large (small) values of κ display a higher (lower) degree of randomness. As it was shown in reference [3], random lattices with different κ are different regularizations of the same theory. In particular, it was shown that the Λ parameter is κ -dependent. In the present paper, we will check this statement by a numerical simulation and, moreover, we will give hints that the non-universal non-leading coefficients of the β function of the model are also κ -dependent.

The level of randomness can be clearly manifested with the distributions of some geometrical properties of the lattice. The first property we plot is the distance of one site to its nearest site, r . This distance, referred to the site i , was written before as r_i . In Figure 5, we show the probability distribution of this distance, $P(r)dr$ for a $\kappa = \infty$ lattice. The histogram in the Figure is the numerical result, obtained by calculating r_i for a single site on 30000 random lattices of 1000 sites. The solid line is the theoretical well known Poisson distribution,

$$P(r)dr = 2\pi \frac{r}{a^2} e^{-\pi r^2/a^2} dr. \quad (2.8)$$

Both curves are normalized to 1 and should coincide.

In Figure 6, we show the same distribution for a $\kappa = 1.3$ random lattice. It was obtained as in Figure 5, with 30000 random lattices of 1000 sites. Notice that the distribution displays less dispersion. The cutoff of the curve is placed at a/κ . Given a random lattice constructed with some finite value of κ , all sites are farther from each other than a/κ . If we bring together two of these sites a distance less than a/κ , the random lattice will not vary its geometrical properties. We checked that the results of the simulations performed on it, do not vary either. Indeed, apart from a tiny bump at some position between $r = 0$ and $r = a/\kappa$, Figure 6 will not change. The more sites the random lattice has, the tinier the bump becomes.

Another quantity we can plot is the distribution of link lengths. In Figure 7 we show the distribution of link lengths $P(l)dl$ for a random lattice with $\kappa = \infty$. Given a site on the lattice, it is always linked with the closest site to it. But it can also be linked with sites placed quite far away. This is why Figures 5 and 7 differ. Finally, in Figure 8 we show the distribution of link lengths for a random lattice with $\kappa = 1.3$. Again we see that the distribution is sharper as κ becomes smaller.

In table 1 we show the numerical average values of link lengths $\langle l \rangle$ and distance between closest sites $\langle r \rangle$ for several values of κ . These quantities can be used to characterize the

degree of randomness. However, our method to construct the random lattice needs only the knowledge of κ as previously explained. Therefore, we will label our random lattices with this κ parameter. The column for $\langle l \rangle$ was obtained averaging the link lengths of random lattices with 10000 sites for $\kappa = \infty$, 1.3 and 1000 sites for $\kappa = 1.2$. The column for $\langle r \rangle$ was calculated by averaging r on a single site for 30000 random lattices of 1000 sites for $\kappa = \infty$ and 1.3; for $\kappa = 1.2$ we averaged on 14 random lattices of 100 sites. The numbers shown depend on the lattice size. As this size gets larger, the averages tend to stabilize. For instance, the averages for $\langle r \rangle / a$ calculated on random lattices of 100, 1000 and 10000 sites with $\kappa = \infty$ are 0.523(2), 0.508(2) and 0.504(2) respectively. The exact value computed from Eq. (2.8) is $\langle r \rangle = \frac{1}{2}a$. The errors shown are only statistical and do not include this systematic effect. The value of $\langle l \rangle$ for $\kappa = \infty$ is known theoretically [11], it is $1.132 a$ in good agreement with the value shown in table 1. The trend shown in Figures 5, 6 and 7, 8 is consistent with the fact that as $\kappa \rightarrow \kappa_{\min}$ the distributions become a Dirac delta. These Dirac deltas are equal and centered at $l, r = \sqrt{2/\sqrt{3}}a \approx 1.0746 a$.

As the number of sites gets larger, all random lattices with a fixed value of κ become equivalent. To support this statement we have generated 100 lattices for several values of L and verified that the average link length presents less standard deviation among the 100 lattices as L becomes greater. If we define $X \equiv D / \langle l \rangle$, where $\langle l \rangle$ is the average link length among the 100 lattices for a fixed value of L and D is the standard deviation of this average, the results are $X = 0.5045, 0.1994, 0.1116, 0.0807 \%$ for $L = 20, 50, 100, 150$ respectively. This analysis was done with $\kappa = \infty$ random lattices.

III. THE SIMULATION ALGORITHM

The best algorithm for the updating of the $O(n)$ non-linear σ -model in a numerical simulation is the non-local Wolff algorithm [10]. On the regular lattice it does not show any critical slowing down. Let τ be the time correlation of the Markov chain of states generated by the algorithm. Let ξ be the spatial correlation length of the model (a well defined function of β). Then, the Wolff algorithm has the fundamental property that τ does not increase as the critical point, corresponding to $\xi = \infty$, is approached.

This nice property is allowed by the intrinsic non locality of the Wolff updating and has nothing to do with the details of the lattice. We argue that it should hold also for the straightforward generalization of the Wolff algorithm on the random lattice. Indeed, our numerical data show that the algorithm performs very well at increasing β , just like in the regular case.

The above mentioned generalization is obtained as follows: we start by choosing at random one lattice site i and an unitary vector $\vec{u} \in S^{n-1}$. There is a great freedom in the

distribution of \vec{u} . To be definite we chose the uniform distribution on the hypersphere by taking at random a point inside the hypercube $\vec{x} \in [0, 1]^n$ and rejecting it if $\|\vec{x}\| > 1$. Then, $\vec{u} = \vec{x} / \|\vec{x}\|$.

We now mark with a label the site i and all of its neighbours according to the probability weights

$$p_{ij} = 1 - \exp \left[\min \left(0, -\frac{2\lambda_{ij}}{g} (\vec{\phi}_i \cdot \vec{u})(\vec{\phi}_j \cdot \vec{u}) \right) \right]. \quad (3.1)$$

We continue recursively from the new marked sites and proceed further until no new site is added to the list of labelled sites.

When the recursive process ends, we collect in a cluster all the marked sites and transform them with a reflection

$$\vec{\phi} \rightarrow R\vec{\phi} \equiv \vec{\phi} - 2(\vec{\phi} \cdot \vec{u})\vec{u}. \quad (3.2)$$

As Wolff has shown [14], in the process of construction of the cluster, all the quantities entering the r.h.s. of

$$\langle \vec{\phi}(x) \cdot \vec{\phi}(y) \rangle = n N \left\langle (\vec{\phi}(x) \cdot \vec{u})(\vec{\phi}(y) \cdot \vec{u}) \frac{1}{|C|} \theta_C(x) \theta_C(y) \right\rangle \quad (3.3)$$

have already been calculated at each updating step. The above expression is called an improved estimator for the two point function. In Eq. (3.3) N is the total number of sites of the lattice, $|C|$ is the number of sites in the cluster and θ_C is the characteristic function of the cluster. Another advantage of this estimator is that it can be measured after each updating step without need of decorrelating updatings.

IV. THE PHYSICAL OBSERVABLES

The physical observables that we have measured are the mass gap for several values of n and the topological charge for $n = 3$. For each of these quantities we have studied the asymptotic scaling behaviour. The universal 2-loop β function of the $O(n)$ non-linear σ -model is

$$\beta(g) = -\frac{n-2}{2\pi} g^2 - \frac{n-2}{4\pi^2} g^3 + O(g^4), \quad (4.1)$$

and therefore the lattice spacing obeys the renormalization group law

$$a\Lambda_{\text{lattice}} = f(\beta) \equiv \left(\frac{2\pi\beta}{n-2} \right)^{1/(n-2)} \exp \left(-\frac{2\pi\beta}{n-2} \right) \left(1 + \mathcal{O}\left(\frac{1}{\beta}\right) \right). \quad (4.2)$$

The first non-universal correction for this scaling function on a regular lattice is known [15]. On the other hand, the value of $\Lambda_{\text{lattice}}/\Lambda_{\overline{\text{MS}}}$ is known both for regular [16] and random lattices [3].

Any dimensionful quantity \mathcal{A} measured on the lattice with the operator \mathcal{A}^L must satisfy (after the subtraction of the relevant mixings)

$$\frac{\mathcal{A}^L}{f(\beta)^{\dim \mathcal{A}}} = \frac{\mathcal{A}}{\Lambda_{\text{lattice}}^{\dim \mathcal{A}}}, \quad (4.3)$$

when $\beta \rightarrow \infty$. Asymptotic scaling holds when the l.h.s. of the above expression, with the first terms of the beta function in $f(\beta)$, depends little on β .

The analytical prediction for the mass gap of the σ model is [6]

$$m = \left(\frac{8}{e}\right)^\Delta \frac{1}{\Gamma(1 + \Delta)} \Lambda_{\overline{\text{MS}}}, \quad \Delta = \frac{1}{n - 2}, \quad (4.4)$$

which combined with the ratio [16]

$$\Lambda_{\text{regular}} = 32^{-1/2} \exp\left(-\frac{\pi\Delta}{2}\right) \Lambda_{\overline{\text{MS}}}, \quad (4.5)$$

gives $m/\Lambda_{\text{regular}}$.

In order to evaluate m we studied the wall-wall correlation function by integrating the two-point function along the spatial direction and studying it at large temporal separations. Notice that on the random lattice the ν -th temporal slice must be defined as the set of sites with $t_\nu < t < t_{\nu+1}$. Moreover, the number of sites that this time slice contains is a function of ν . This is a source of systematic error. As N , the total number of sites, gets larger, the width of the time slice $t_{\nu+1} - t_\nu$ can be smaller and reduce the previous systematic error.

Numerical studies on the regular lattice indicate that a fit of the wall-wall correlation Monte Carlo data to the behaviour

$$C(t) \equiv A \cosh\left[B\left(t - \frac{L}{2}\right)\right] \quad (4.6)$$

is enough to reproduce the data [14]. To avoid correlation among data at different t , we used sets of different runs for every t . Hence, the statistical errors obtained are reliable.

The above mentioned improved estimator, Eq. (3.3), reduces greatly the statistical noise which affects this measure particularly at large t .

We have also measured the topological charge and susceptibility of the $O(3)$ model on a random lattice. The topology of this model is based on the stereographic map from the sphere S^2 onto the projective plane [5]. The topological charge actually counts the winding or instanton number of this mapping on classical configurations. In the continuum it is defined as

$$Q = \int d^2x Q(x), \quad Q(x) = \frac{1}{8\pi} \epsilon_{\mu\nu} \epsilon_{abc} \phi^a(x) \partial_\mu \phi^b(x) \partial_\nu \phi^c(x), \quad (4.7)$$

and it rigorously yields integer values on a smooth field configuration. At the quantum level, Q is a composite operator which requires a renormalization procedure.

On a random lattice, we introduce the following definition of topological charge at the site i

$$Q_i = \frac{1}{32\pi} \sum_{j,k} \frac{\lambda_{ij} \lambda_{ik}}{\omega_i} \epsilon_{abc} \phi_i^a \phi_j^b \phi_k^c \sigma_{ijk} \quad (4.8)$$

which, by using Eqs. (2.5) and (2.6), reproduces the continuum expression, Eq. (4.7). On a regular lattice, where $\mathbf{d}_{ij} = \mathbf{0}$, \mathbf{l}_{ij} is equal either to $\hat{\mathbf{x}}$ or to $\hat{\mathbf{y}}$ and λ_{ij} is 1 for linked sites and 0 otherwise, Eq. (4.8) reproduces the standard definition [17]. The total topological charge Q is calculated just by $Q = \sum_i Q_i$.

An interesting and non-trivial quantity which can be extracted from the topological charge is the topological susceptibility which in the continuum is defined as the two point correlation of the topological charge at zero external momentum

$$\chi \equiv \int d^2x \langle Q(x) Q(0) \rangle. \quad (4.9)$$

On the lattice, this is rewritten in the following way

$$\chi^L = \frac{1}{V} \left\langle \left(\sum_i Q_i \right)^2 \right\rangle. \quad (4.10)$$

The Monte Carlo data for the topological susceptibility χ^L is [17]

$$\chi^L = a^2(\beta) Z(\beta)^2 \chi + a^2(\beta) A(\beta) \langle S(x) \rangle_{NP} + P(\beta), \quad (4.11)$$

where $a(\beta) = f(\beta)/\Lambda_{\text{lattice}}$, Eq. (4.2), $\langle S(x) \rangle_{NP}$ is the non-perturbative vacuum expectation value of the density of action and $Z(\beta)$, $A(\beta)$ and $P(\beta)$ are the renormalizations which can be calculated perturbatively [17,18]. On the regular lattice $\langle S(x) \rangle_{NP}$ is negligible [19] and so is the second term in the r.h.s. of Eq. (4.11). We have not calculated all of these renormalizations on the random lattice but instead we have used the cooling method [7]. The cooling procedure is a relaxation process which after a few cooling steps (~ 30 – 40 steps) have almost eliminated all short scale fluctuations leaving the long waves still present. If we assume that these short scale fluctuations, of order $\mathcal{O}(a)$, are responsible for the quantum noise which shows up as renormalization effects, then after some cooling steps all renormalizations in Eq. (4.11) will disappear and the physical and Monte Carlo topological susceptibility will be related by the expression

$$\chi = \frac{\chi^L}{a(\beta)^2}. \quad (4.12)$$

However the situation for the $O(3)$ σ model is not so simple. In this model, instantons tend to be small. Indeed the distribution of instantons with radius ρ in this theory satisfies $d\mathcal{N}/d\rho \propto 1/\rho$. As a consequence, the previous cooling process can also eliminate small $\mathcal{O}(a)$ instantons, thus modifying the topological content of the configuration. This unwanted behaviour of the cooling occurs on regular lattices [19]. On a random lattice some sites can group together forming clusters with a typical size less than one lattice spacing. This fact happens mostly on large κ lattices (see Figure 4). This geometry might allow the existence of very small instantons with a size $\rho \ll a$. This is the main motivation for studying the topological properties of the model on random lattices.

In Figure 9 we show the evolution of the topological charge for 40 uncorrelated configurations as the cooling process goes on. At zero cooling step the value of the charge on the lattice is on average $Q^L = QZ(\beta)$. Instead, after 30 or 40 steps, this charge reached an almost integer value which depends only on the underlying instantonic content of the original configuration. This almost integer value remains stable for a long plateau. Thus, we assumed the value of Q^L after 30 or 40 steps of cooling as the correct topological charge of the configuration. We checked that the value of the topological susceptibility is also stable on the plateau. Indeed, the value obtained is within errors, the same if 30, 40 or 50 cooling steps are performed. It can also be seen from Figure 9 that the value of Q^L after several coolings is not exactly an integer. This is a general fact and has to do with the fact that instantons are not exact solutions of the theory defined on a lattice. We also checked that the susceptibility is insensitive to rounding this number to its nearest integer. We chose for our analysis the values of Q^L after 30 cooling steps without rounding it to the nearest integer.

We now turn to a detailed description of the cooling step. It consists in locally minimizing the action with respect to the field at each site once per step. We used a controlled cooling [8]. This means that for a given positive number δ , the new field $\vec{\phi}'_i$ and the old one $\vec{\phi}_i$ differ less than δ , $\|\vec{\phi}_i - \vec{\phi}'_i\| \leq \delta$. First we define the force relative to the site i as

$$\vec{F}_i \equiv \frac{\sum_j \lambda_{ij} \vec{\phi}_j}{\|\sum_j \lambda_{ij} \vec{\phi}_j\|}, \quad (4.13)$$

and then we compute the distance between the force and the field at this site i , $d \equiv \|\vec{F}_i - \vec{\phi}_i\|$. Now, if $d \leq \delta$ then the new field is going to be $\vec{\phi}'_i = \vec{F}_i$. Instead, if $d > \delta$ then the field at the site i becomes

$$\vec{\phi}'_i = \frac{\vec{\phi}_i + \epsilon (\vec{F}_i - \vec{\phi}_i)}{\|\vec{\phi}_i + \epsilon (\vec{F}_i - \vec{\phi}_i)\|}, \quad (4.14)$$

where ϵ is chosen to be

$$\epsilon \equiv \frac{\delta}{d\sqrt{1 - \frac{1}{4}d^2}}. \quad (4.15)$$

In a step of cooling we pass through all sites i of the lattice and perform the previous modification on the corresponding field $\vec{\phi}_i$.

V. THE MONTE CARLO RESULTS

In this section we will show the set of Monte Carlo data obtained for the mass gap and the topological susceptibility and discuss their consequences.

In table 2 we show the set of data for the mass gap and the $O(3)$ σ model on lattices of 200^2 sites. They are also shown in Figure 10. The data were obtained from 12000 measures of the improved correlator, Eq. (3.3) for each β . We fit these data to the scaling function of Eq. (4.2)

$$f(\beta) = 2\pi\beta\alpha_1 \exp(-2\pi\beta\alpha_2), \quad (5.1)$$

where α_1 and α_2 are the parameters of the fit. In particular, α_2 must be equal to 1 in order for the data to scale as the β function of the theory predicts, Eq. (4.1), and α_1 must be $m/\Lambda_{\text{lattice}}$.

The fit gives $\alpha_2 = 1.02(2)$, $0.97(2)$, $0.95(2)$ for the regular lattice, $\kappa = 1.3$ and $\kappa = \infty$ random lattices respectively. This is in agreement with the result of [3] concerning the universality of the random lattice: the first coefficient of the beta function is the same in any lattice regularization. Now, imposing $\alpha_2 = 1$ and leaving α_1 free we obtained $\alpha_1 = 121(2)$, $139(2)$, $91(1)$ for regular lattice, $\kappa = 1.3$ and $\kappa = \infty$ random lattice respectively, with a value for $\chi^2/\text{n.d.f.}$ equal to $6/11$, $8/11$ and $9/12$ respectively. Following [6] and [3], the expected results for α_1 are 80.09, 87.05 and 44.49 respectively. We excluded any finite size explanation to this discrepancy. We arrived at this conclusion because *a*) the technique of reference [20] did not improve the results and *b*) the fits with the data of table 3 for 400^2 lattices yielded similar results for α_1 . We think that the disagreement is due to the fact that our range of β is narrow enough to collect into α_1 all the power-law corrections to the asymptotic scaling function. Unfortunately, another single free parameter is not able to account for the whole non-universal terms correcting Eq. (5.1) and it did not improve dramatically the result for α_1 .

From the results of the fits for α_1 we can get the ratio between Λ parameters. Let us define $R(\kappa) = \Lambda_{\text{random}}/\Lambda_{\text{regular}}$ at a given κ . Then, $R(1.3) = 0.87(3)$ and $R(\infty) = 1.33(4)$. These results are in agreement with the average of the ratios obtained from each β : $R(1.3) = 0.86(6)$ and $R(\infty) = 1.29(8)$. These ratios for each β are shown in Figure 11. The theoretical values [3] are $R(1.3) = 0.92(2)$ and $R(\infty) = 1.8(2)$. For $\kappa = 1.3$ theoretical and Monte Carlo ratios are in agreement within errors. But this is not so for $\kappa = \infty$. We again think that this is due to the lack of asymptotic scaling.

It is well known that asymptotic scaling is rather elusive in the $O(3)$ σ model and here we have realised that this problem does not ameliorate if a random lattice is used. For this reason, we also performed runs for the $O(4)$ and $O(8)$ models where it is known that asymptotic scaling is better achieved [9]. In table 4 the mass gap data for $O(4)$ on lattices with 400^2 sites are shown. In table 5 the same data are shown for $O(8)$ and lattices with 300^2 sites. In both cases 12000 measures of the improved estimator, Eq. (3.3), were performed for each β .

The $O(4)$ data of table 4 were fitted to

$$f(\beta) = \sqrt{\pi\beta\alpha_1} \exp(-\pi\beta\alpha_2). \quad (5.2)$$

The result for α_2 was again close to 1: 1.02(4), 1.05(7) and 1.04(4) for regular, $\kappa = 1.3$ and $\kappa = \infty$ random lattices respectively. Fixing α_2 to 1, we obtained for α_1 26.6(5), 28.4(9) and 22.3(4) for regular, $\kappa = 1.3$ and $\kappa = \infty$ random lattices respectively, while the predicted values are [3,6] 24.02, 25.55 and 16.01. We see a much better agreement between theoretical and Monte Carlo results. The ratio of Λ parameters extracted from the Monte Carlo data is $R(1.3) = 0.94(5)$ and $R(\infty) = 1.20(4)$. The theoretical ratios are [3] 0.94(2) and 1.5(1) respectively. The agreement for $\kappa = \infty$ is still not satisfactory.

The data of table 5 for $O(8)$ were fitted to

$$f(\beta) = \left(\frac{\pi\beta}{3}\right)^{1/6} \alpha_1 \exp\left(-\frac{\pi\beta\alpha_2}{3}\right). \quad (5.3)$$

Again α_2 was satisfactorily close to 1. The fit for α_1 shows a good asymptotic scaling ($\alpha_1 = 10.0(4)$ for the regular lattice while Eqs. (4.4) and (4.5) give 9.48). So we expect that this time the ratios of Λ parameters extracted from Monte Carlo will be in agreement with the theoretical ones. The Monte Carlo ratios are $R(1.3) = 0.90(6)$ and $R(\infty) = 1.29(9)$. The theoretical ratios are 0.95(2) and 1.3(1) respectively.

We conclude that the dependence of the Λ parameter on κ , the degree of randomness of the lattice, is qualitatively correct. The figures shown in [3] for these ratios are also correct but the lack of asymptotic scaling prevent us from checking them for the $O(n)$ model when $n \leq 6-8$.

Let us now discuss the results for the topological susceptibility obtained for the $O(3)$ model. In table 6 we show χ^L after 30 cooling steps which, as described in section 4, equals $a^2\chi$. These data have been obtained on lattices with 200^2 sites performing the cooling process on 1000 uncorrelated configurations for each β . In Figure 12 we show this set of data for the three kinds of lattices used and the result of the fits performed on it by imposing the scaling function Eq. (5.1) with $\alpha_2 = 1$. It is apparent that the data do not scale as Eq. (5.1) imposes.

If α_2 is left free, we see again that the data do not scale as they should. Indeed, for the regular lattice, $\kappa = 1.3$ and $\kappa = \infty$ random lattices, we obtain $\alpha_2 = 0.70(4)$, $0.64(4)$, $0.69(4)$

respectively. We repeated the same analysis on larger lattices to check whether this discrepancy is due to finite size effects on the data. In table 7 we show the data for a regular lattice with 300^2 sites and in table 8 the data for a $\kappa = \infty$ random lattice with 400^2 sites. They are also obtained by cooling 1000 uncorrelated configurations. The fit on the data of table 7 gives $\alpha_2 = 0.76(4)$ and the fit on table 8 $\alpha_2 = 0.65(4)$. From these figures we could hardly conclude that the lack of correct scaling is due to finite size effects. We think that this problem must be traced back to the elimination of small instantons during the cooling process. Probably, the use of large κ random lattices is not enough to avoid this effect.

The lack of asymptotic scaling prevented us from using the topological susceptibility and the mass gap data to check the physical scaling of the $O(3)$ model on random lattices.

In Figure 13 we show the ratio of Λ parameters for each value of β from the data of the topological susceptibility. The average result for this ratio is surprisingly similar to the one obtained from the mass gap data: $R(1.3) = 0.94(2)$ and $R(\infty) = 1.37(3)$.

VI. CONCLUSIONS

We have used the random lattice to simulate the 2-dimensional $O(n)$ non-linear σ -model. The sites of the random lattice are considered as the centers of hard spheres of radius $a/2\kappa$ where a is the lattice spacing. These hard spheres are located at random on the lattice volume. The links between neighbouring sites are established by a well known triangularization process [12].

To compare the performance of different lattices, we made the simulations on regular lattices and random lattices with both $\kappa = 1.3$ and $\kappa = \infty$.

We used the Wolff algorithm [10] for the simulations as well as an improved estimator [14] for the computation of two-point correlation functions. We measured the mass gap (as the inverse of the correlation length measured from the wall-wall two-point correlation function) and the topological susceptibility. The topological charge was calculated by using a cooling technique [7] and we introduced a regularized operator for the topological charge on the lattice (see Eq. (4.8)).

The Monte Carlo results for the mass gap scale as they should, confirming previous claims [3] about the universality of the random lattice regularization. They do not present any finite size problems (for 200^2 sites) but for small values of n the asymptotic scaling is not fulfilled. For the $O(8)$ model, where the data display a good asymptotic scaling, we can reproduce the theoretical value for the ratio between Lambda parameters $\Lambda_{\text{random}}/\Lambda_{\text{regular}}$ for $\kappa = \infty$, thus confirming the semi-analytical prediction of reference [3]. Instead, for $\kappa = 1.3$, the Monte Carlo value for the previous ratio is in good agreement with the theoretical prediction already in the $O(3)$ model. This could mean that both regularizations (regular

lattice and $\kappa = 1.3$ random lattice) are quite similar and in particular the non-universal terms in the scaling function, Eq. (4.2), almost coincide. This assumption is also supported by the fact that $\Lambda_{\text{random}}/\Lambda_{\text{regular}}$ for $\kappa = 1.3$ is close to 1. In any case, these conclusions are consistent with the scenario where also the non-universal terms in the scaling function, Eq. (4.2) are κ -dependent.

The data for the topological susceptibility scale very badly. We think that the cooling process removes small instantons thus modifying the topological content of the configuration also on random lattices. The cooling smooths out fluctuations with a length of order $\mathcal{O}(a)$. For smaller β the lattice spacing is longer in physical units, therefore the number of eliminated instantons when smoothing out $\mathcal{O}(a)$ fluctuations is also larger. This explains why the data in Figure 12 and Tables 6,7 and 8 are shifted downwards for small β .

In any case, our results prove that the semi-analytical method used in reference [3] is reliable to perform analytical calculations on random lattices.

VII. ACKNOWLEDGEMENTS

We thank Federico Farchioni and Andrea Pelissetto for useful discussions. We also acknowledge financial support from INFN.

REFERENCES

- [1] Z. Qiu, H. C. Ren, X. Q. Wang, Z. X. Yang and E. P. Zhao, Phys. Lett. **B198** (1987) 521; **B203** (1988) 292.
- [2] Work in progress.
- [3] B. Allés, Nucl. Phys. **B437** (1995) 627.
- [4] A. M. Polyakov, Phys. Lett. **B59** (1975) 79; E. Brézin and J. Zinn-Justin, Phys. Rev. **B14** (1976) 3110.
- [5] A. A. Belavin and A. M. Polyakov, JETP Letters **22** (1975) 245.
- [6] P. Hasenfratz, M. Maggiore and F. Niedermayer, Phys. Lett. **B245** (1990) 522; P. Hasenfratz and F. Niedermayer, Phys. Lett. **B245** (1990) 529.
- [7] E. M. Ilgenfritz, M. L. Laursen, M. Müller-Preussker, G. Schierholz and H. Shiller, Nucl. Phys. **B268** (1986) 693; M. Teper, Phys. Lett. **B171** (1986), 81, 86; J. Hoek, M. Teper and J. Waterhouse, Phys. Lett. **B180** (1986) 112; Nucl. Phys. **B288** (1987) 589.
- [8] M. Campostrini, A. Di Giacomo, H. Panagopoulos and E. Vicari, Nucl. Phys. **B329** (1990) 683.
- [9] U. Wolff, Phys. Lett. **B248** (1990) 335.
- [10] U. Wolff, Phys. Rev. Lett. **62** (1989) 361.
- [11] N. H. Christ, R. Friedberg and T. D. Lee, Nucl. Phys. **B202** (1982) 89.
- [12] R. Friedberg and H. C. Ren, Nucl. Phys. **B235** [FS11] (1984) 310.
- [13] N. H. Christ, R. Friedberg and T. D. Lee, Nucl. Phys. **B210** (1982) 337.
- [14] U. Wolff, Nucl. Phys. **B334** (1990) 581.
- [15] M. Falcioni and A. Treves, Nucl. Phys. **B265** [FS15] (1986) 671.
- [16] G. Parisi, Phys. Lett. **B92** (1980) 133.
- [17] A. Di Giacomo, F. Farchioni, A. Papa and E. Vicari, Phys. Rev. **D46** (1992) 4630.
- [18] A. Di Giacomo, F. Farchioni, A. Papa and E. Vicari, Phys. Lett. **B276** (1992) 148.
- [19] F. Farchioni and A. Papa, Nucl. Phys. **B431** (1994) 686.
- [20] M. Lüscher in “Progress in gauge field theory” (Cargèse 1983), G. 't Hooft et al. (eds.), Plenum, New York (1984); I. Bender and W. Wetzel, Nucl. Phys. **B269** (1986) 389.

Figure captions

- Figure 1. Location of hard discs for a lattice of 3^2 sites with $\kappa = 1$. The radius of the discs is equal to $a/2$. In a) it corresponds to a regular square lattice. In b) a column has been shifted: κ still equals 1 but the lattice is no longer regular.
- Figure 2. Location of hard discs for a regular hexagonal lattice with 9 sites. They fit tight and no movement is allowed without breaking the hard nature of the discs.
- Figure 3. The ratio between the number of proposed sites N_p and total number of sites N in the construction of a random lattice as a function of κ . The solid and dashed lines are the results for lattices with $N = 100$ and $N = 1000$ sites respectively.
- Figure 4. The result of the triangularization process performed on two random lattices of 10^2 sites for a) $\kappa = \infty$ and b) $\kappa = 1.3$. The different level of randomness is apparent.
- Figure 5. Distribution probability of distances between a site and its closest neighbour on a random lattice with $\kappa = \infty$. The a in abscisses stands for one lattice spacing. The histogram is the numerical result calculated by using a single site on 30000 random lattices of 1000 sites. This histogram should coincide with the Poisson distribution, shown in the figure with a solid line. Both curves are normalized to 1.
- Figure 6. Distribution probability of distances between a site and its closest neighbour on a random lattice with $\kappa = 1.3$. The a in abscisses stands for one lattice spacing. The histogram is the numerical result calculated by using a single site on 30000 random lattices of 1000 sites. The curve is normalized to 1.
- Figure 7. Distribution probability of link lengths on a random lattice calculated with $\kappa = \infty$. The a in abscisses stands for one lattice spacing. The curve is normalized to 1.
- Figure 8. Distribution probability of link lengths on a random lattice calculated with $\kappa = 1.3$. The a in abscisses stands for one lattice spacing. The curve is normalized to 1.
- Figure 9. Evolution of the measured topological charge along with 50 cooling steps for 40 uncorrelated configurations. Notice the clustering towards integer values after a few coolings. A random lattice with 40^2 sites and $\kappa = \infty$ was used at $\beta = 1.4$.
- Figure 10. Monte Carlo data for the mass gap on a lattice with 200^2 sites. The lines are the results of the fits performed on the Monte Carlo data (shown with circles, squares and diamonds). The solid line (circles), dashed line (squares) and dot dashed line

(diamonds) correspond to the regular lattice, $\kappa = 1.3$ random lattice and $\kappa = \infty$ random lattice respectively.

Figure 11. Ratio of Λ parameters as obtained from the Monte Carlo data of the mass gap. The solid line (squares) and dashed line (circles) correspond to $\kappa = 1.3$ and $\kappa = \infty$ respectively. The average ratios are $\Lambda_{\text{random}}/\Lambda_{\text{regular}}(\kappa = 1.3) = 0.86(6)$ and $\Lambda_{\text{random}}/\Lambda_{\text{regular}}(\kappa = \infty) = 1.29(8)$.

Figure 12. Monte Carlo data for the topological susceptibility on a lattice with 200^2 sites. The lines are the results of the fits performed on the Monte Carlo data (shown with circles, squares and diamonds). The solid line (circles), dashed line (squares) and dot dashed line (diamonds) correspond to the regular lattice, $\kappa = 1.3$ random lattice and $\kappa = \infty$ random lattice respectively.

Figure 13. Ratio of Λ parameters as obtained from the Monte Carlo data of the topological susceptibility. The solid line (squares) and dashed line (circles) correspond to $\kappa = 1.3$ and $\kappa = \infty$ respectively. The average ratios are $\Lambda_{\text{random}}/\Lambda_{\text{regular}}(\kappa = 1.3) = 0.94(2)$ and $\Lambda_{\text{random}}/\Lambda_{\text{regular}}(\kappa = \infty) = 1.37(3)$.

Table captions

Table 1. Average values for the distance between a site and its closest neighbour, $\langle r \rangle$ and the link length $\langle l \rangle$ in units of lattice spacing a for several values of κ . These numbers have been calculated numerically.

Table 2. Monte Carlo data for the mass gap, ma^2 for regular and random lattices with 200^2 sites for the $O(3)$ σ model.

Table 3. Monte Carlo data for the mass gap, ma^2 for regular and random lattices with 400^2 sites for the $O(3)$ σ model.

Table 4. Monte Carlo data for the mass gap, ma^2 for regular and random lattices with 400^2 sites for the $O(4)$ σ model.

Table 5. Monte Carlo data for the mass gap, ma^2 for regular and random lattices with 300^2 sites for the $O(8)$ σ model.

Table 6. Monte Carlo data for the topological susceptibility, $10^4 a^2 \chi$ for regular and random lattices with 200^2 sites for the $O(3)$ σ model.

Table 7. Monte Carlo data for the topological susceptibility, $10^4 a^2 \chi$ for a regular lattice with 300^2 sites for the $O(3)$ σ model.

Table 8. Monte Carlo data for the topological susceptibility, $10^4 a^2 \chi$ for a $\kappa = \infty$ random lattice with 400^2 sites for the $O(3)$ σ model.

Table 1

κ	$\langle l \rangle / a$	$\langle r \rangle / a$
∞	1.131(2)	0.508(2)
1.3	1.113(1)	0.857(1)
1.2	1.109(1)	0.90(2)

Table 2

β	regular	$\kappa = 1.3$	$\kappa = \infty$
1.45	–	–	0.0884(27)
1.5	0.0918(32)	0.1018(30)	0.0656(25)
1.55	0.0716(23)	0.0750(29)	0.0527(31)
1.575	0.0616(30)	0.0759(23)	0.0462(25)
1.6	0.0505(25)	0.0595(22)	0.0390(20)
1.625	0.0480(12)	0.0522(20)	0.0346(21)
1.65	0.0379(18)	0.0471(27)	0.0301(16)
1.675	0.0350(8)	0.0397(30)	0.0260(17)
1.7	0.0284(19)	0.0333(9)	0.0228(15)
1.725	0.0243(16)	0.0298(9)	0.0200(7)
1.75	0.0213(14)	0.0266(7)	0.0171(14)
1.775	0.0191(6)	0.0227(7)	0.0155(13)
1.8	0.0175(12)	0.0190(6)	0.0140(6)

Table 3

β	regular	$\kappa = 1.3$	$\kappa = \infty$
1.6	0.0598(17)	–	0.0438(20)
1.65	0.0393(13)	–	0.0314(20)
1.7	0.0290(12)	–	0.0231(10)
1.75	0.0215(9)	0.0252(11)	0.0170(9)
1.775	0.0184(7)	0.0228(9)	0.0137(4)
1.8	0.0153(6)	0.0191(10)	0.0123(8)

Table 4

β	regular	$\kappa = 1.3$	$\kappa = \infty$
2.4	0.0386(14)	0.0426(33)	0.0333(12)
2.5	0.0313(17)	0.0320(22)	0.0248(11)
2.6	0.0211(9)	0.0228(16)	0.0179(8)
2.7	0.0165(7)	0.0165(12)	0.0129(6)
2.8	0.0117(4)	0.0126(9)	0.0099(5)

Table 5

β	regular	$\kappa = 1.3$	$\kappa = \infty$
4.6	0.1549(163)	0.1663(217)	0.0872(26)
5.2	0.0592(36)	0.0658(21)	0.0471(25)
5.8	0.0287(16)	0.0320(15)	0.0247(14)

Table 6

β	regular	$\kappa = 1.3$	$\kappa = \infty$
1.575	2.90(13)	3.13(14)	1.511(65)
1.6	2.45(10)	2.85(13)	1.252(53)
1.625	1.97(9)	2.16(10)	1.078(51)
1.65	1.61(8)	1.89(10)	0.838(37)
1.675	1.38(6)	1.60(8)	0.741(33)

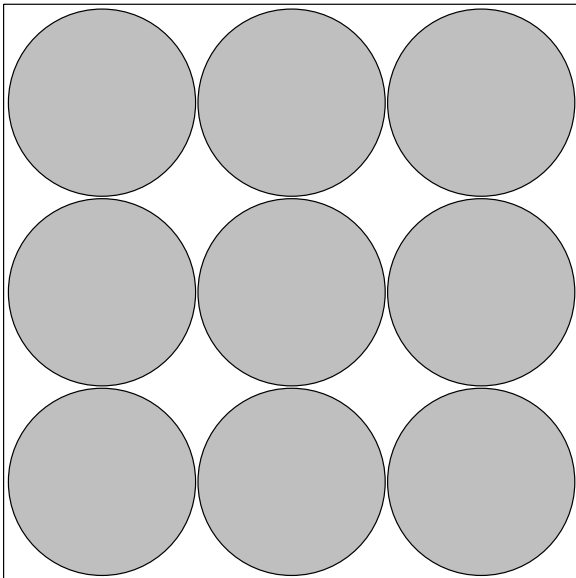
Table 7

β	regular
1.575	2.99(13)
1.6	2.50(11)
1.625	1.96(9)
1.65	1.51(7)
1.675	1.37(6)

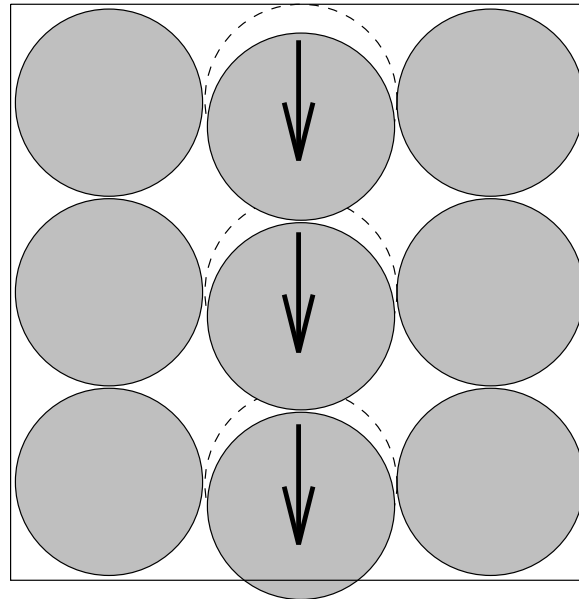
Table 8

β	$\kappa = \infty$
1.575	1.515(66)
1.6	1.307(79)
1.625	1.159(96)
1.65	0.939(41)
1.675	0.747(35)

Figure 1



a)



b)

Figure 2

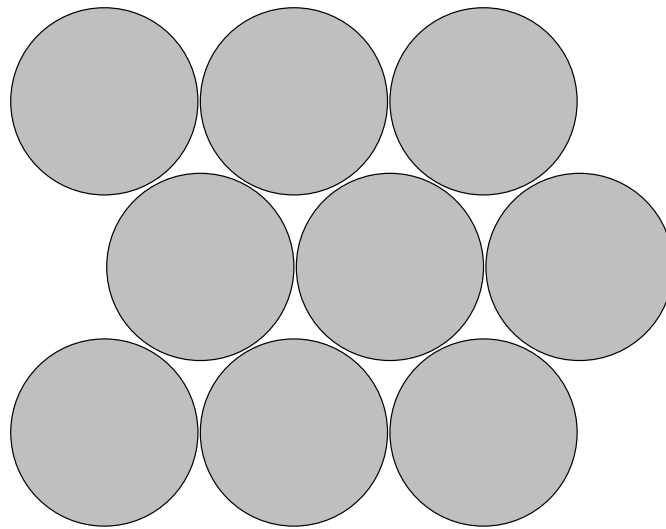


Figure 3

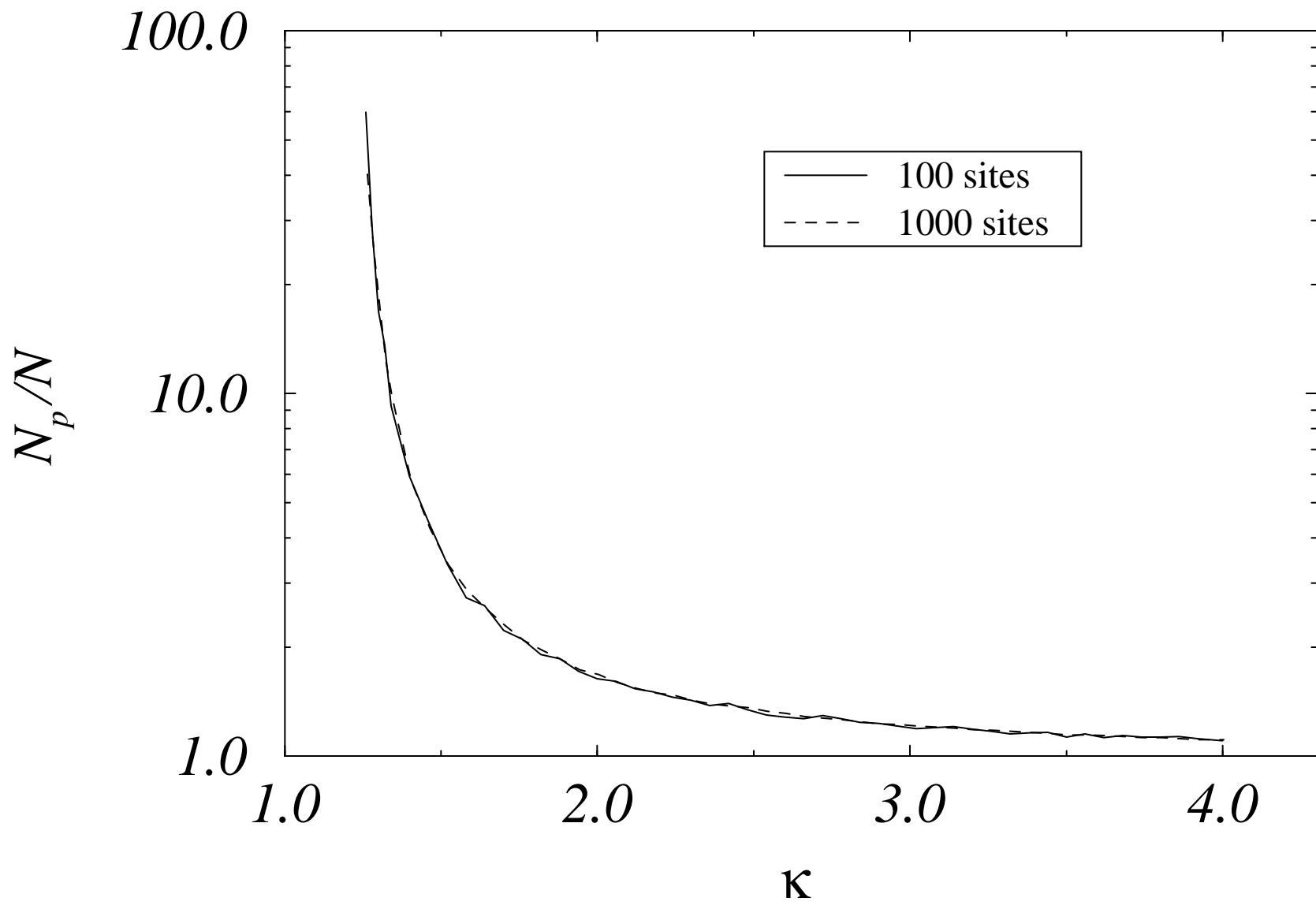
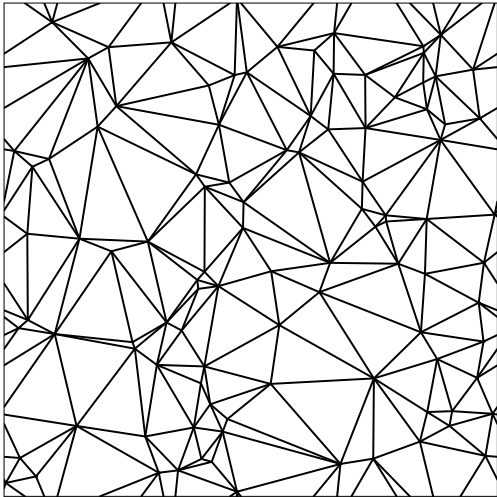
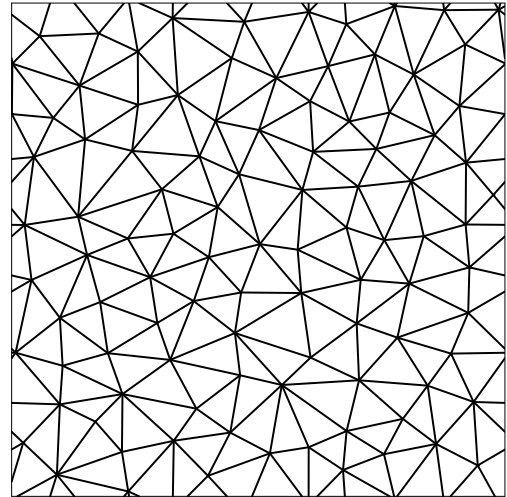


Figure 4



a)



b)

Figure 5

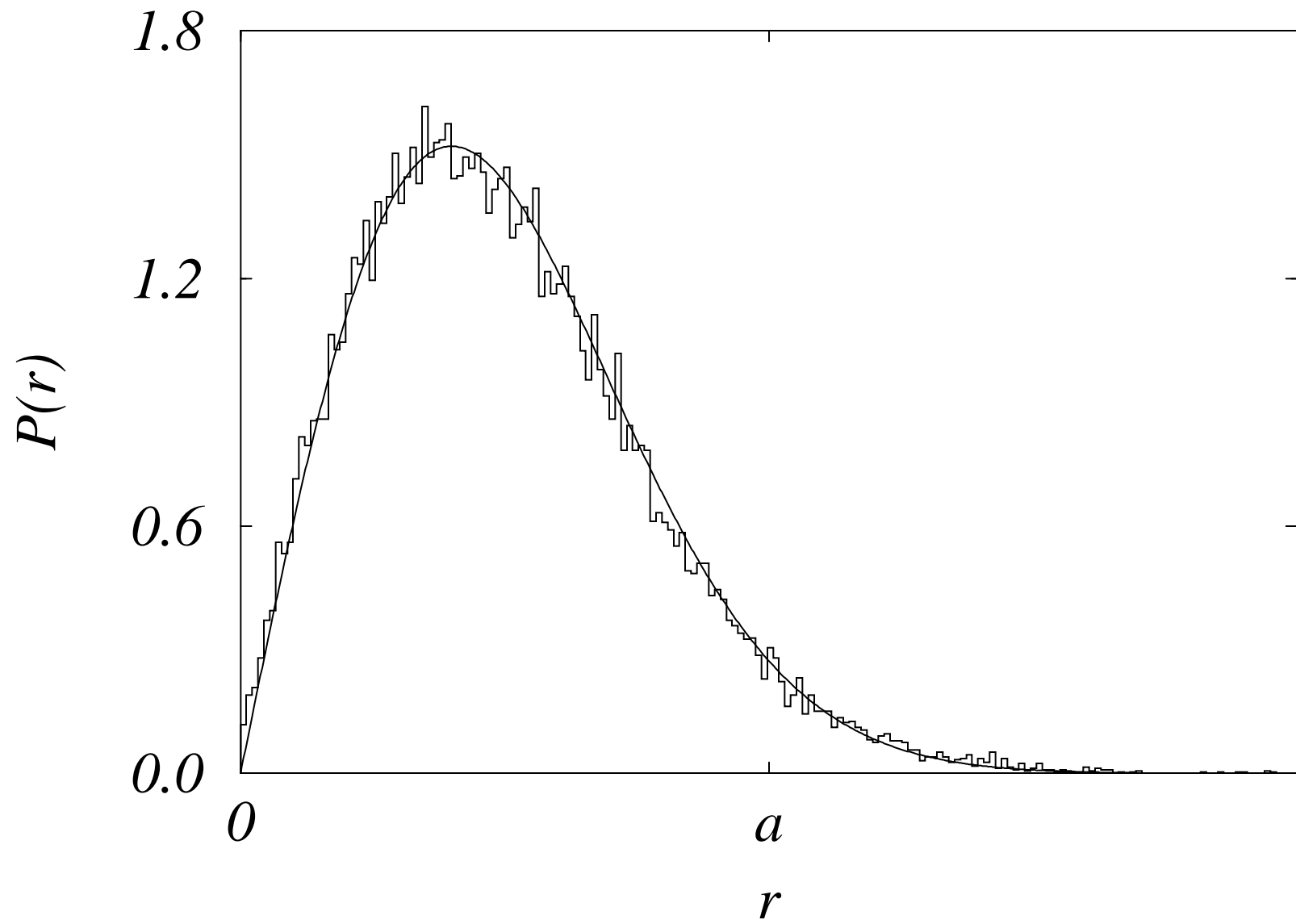


Figure 6

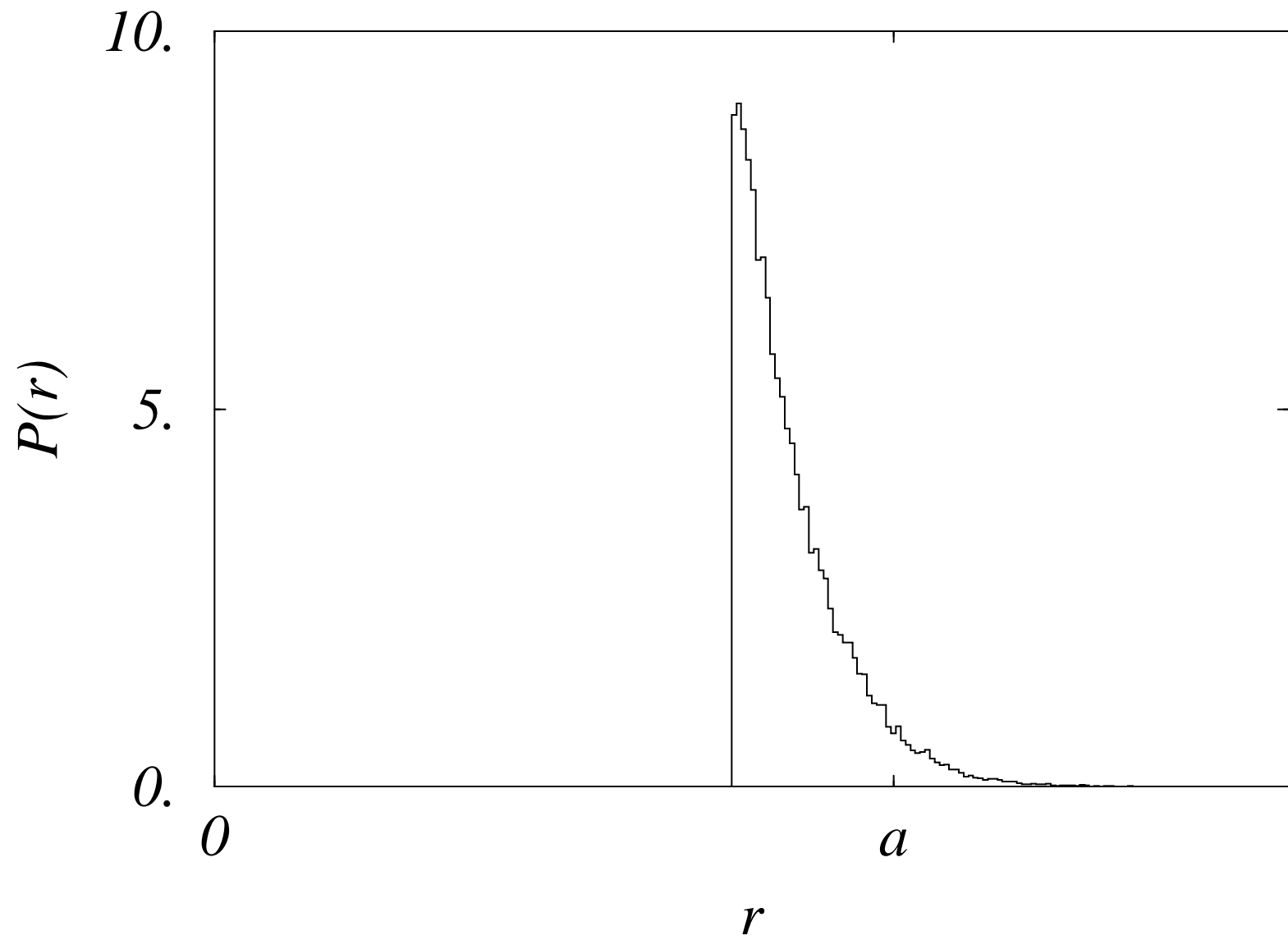


Figure 7

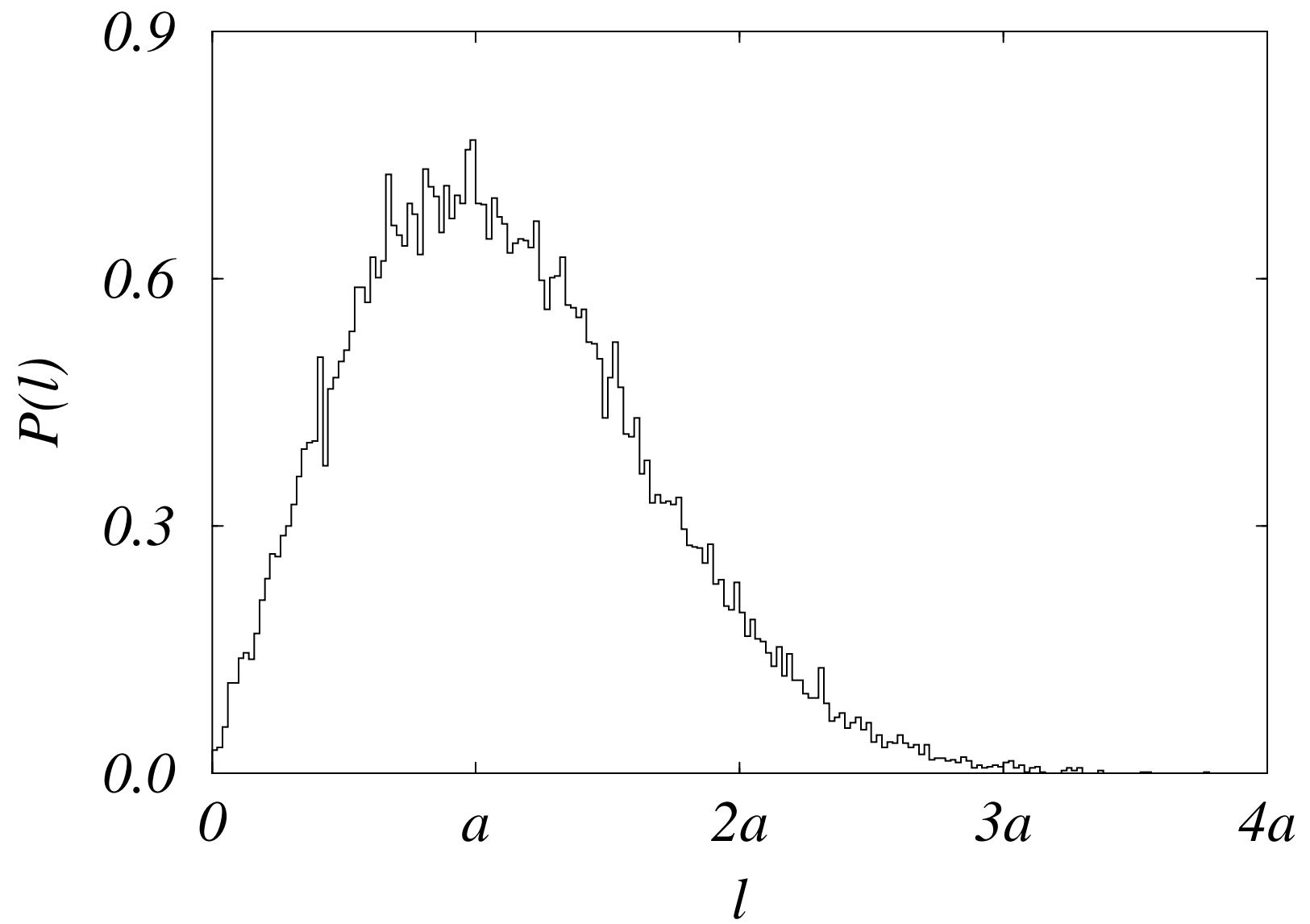


Figure 8

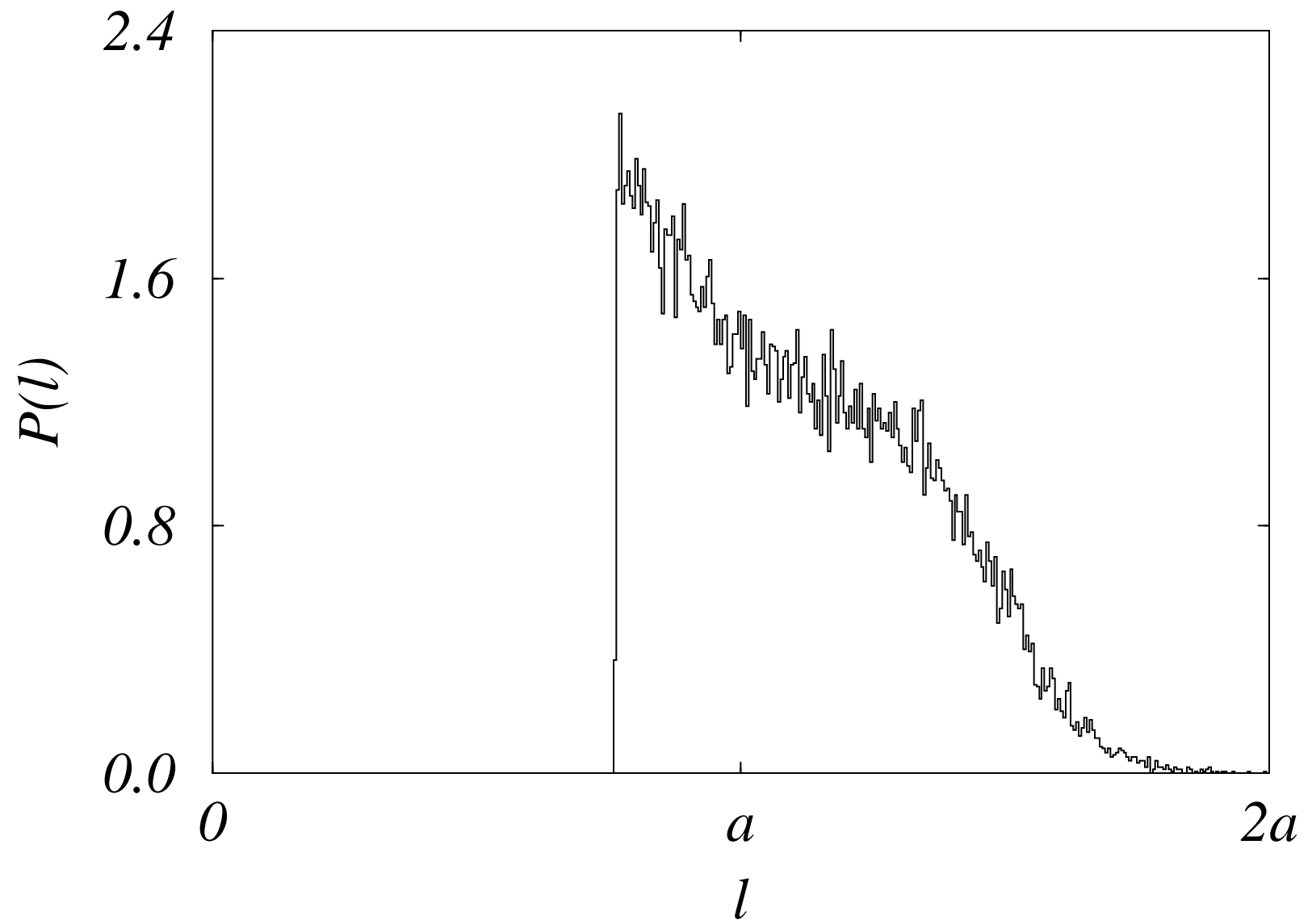


Figure 9

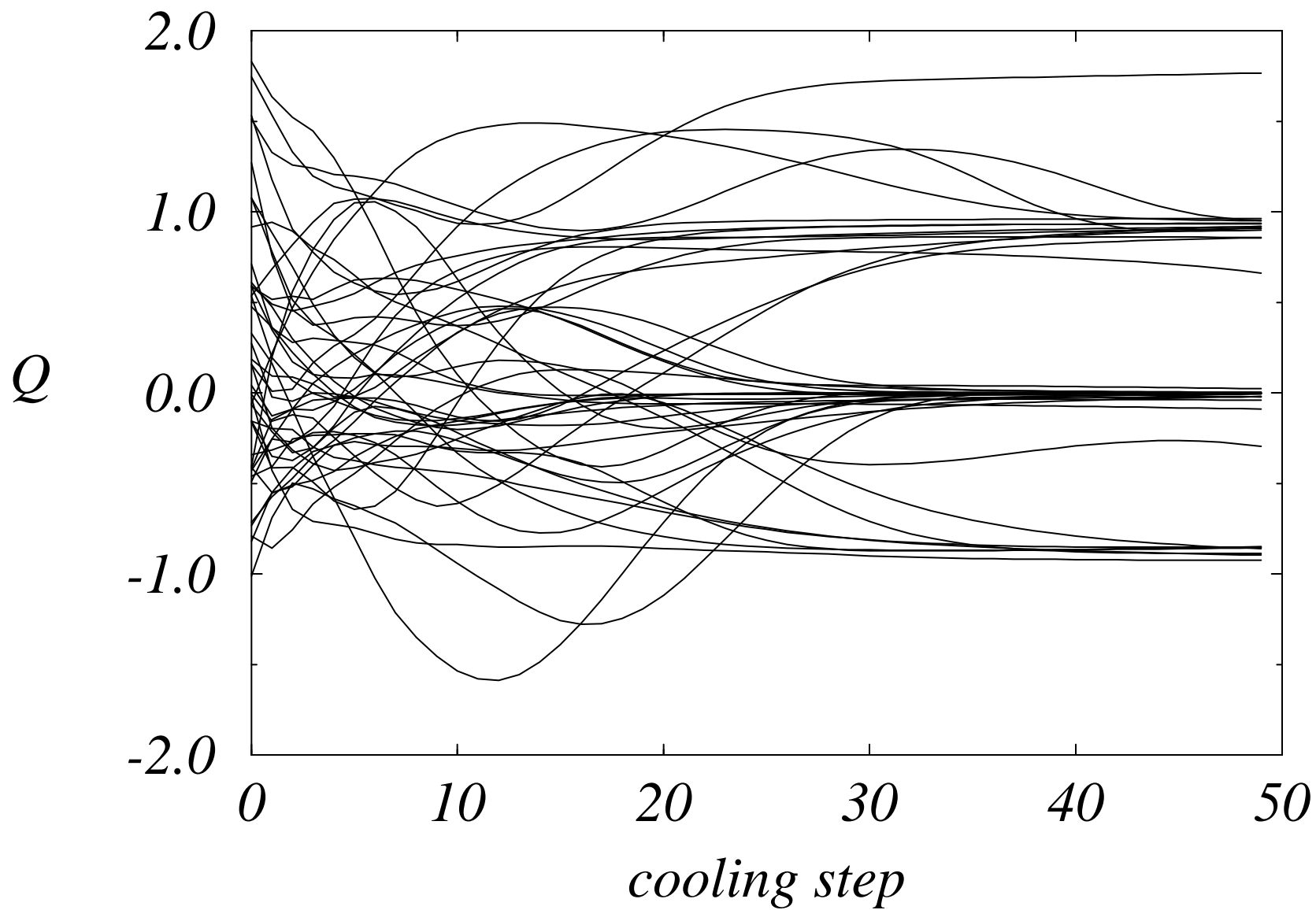


Figure 10

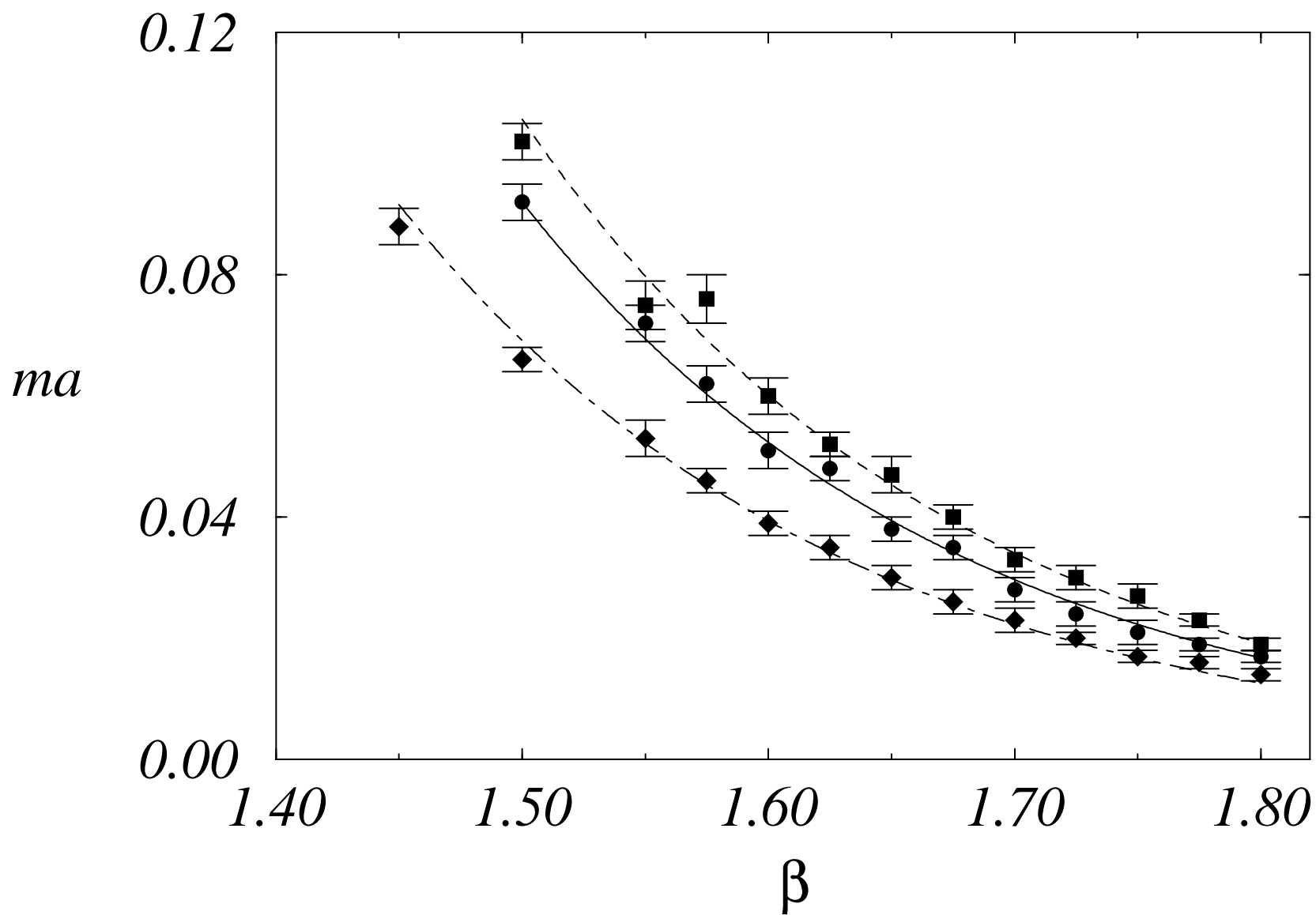


Figure 11

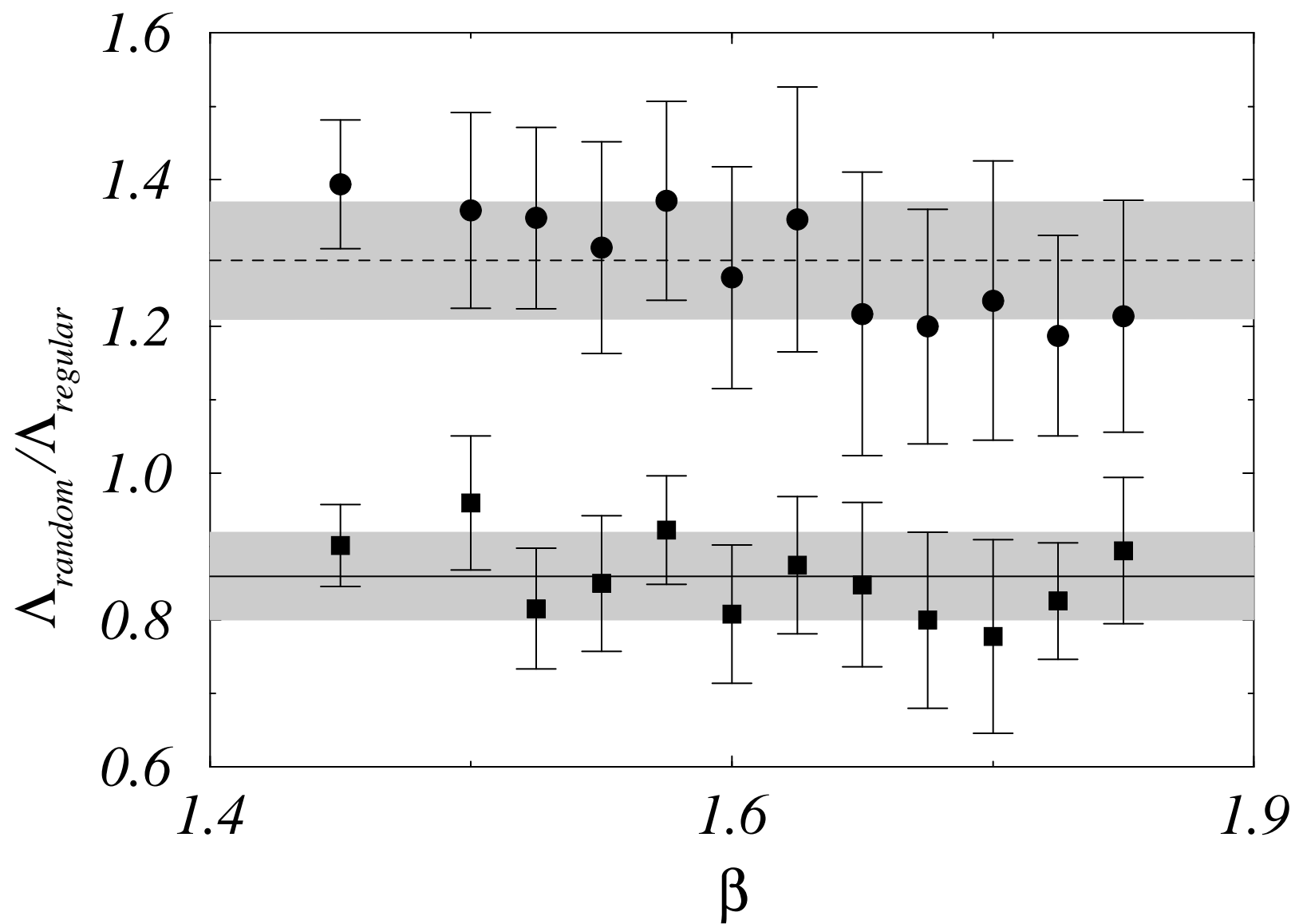


Figure 12

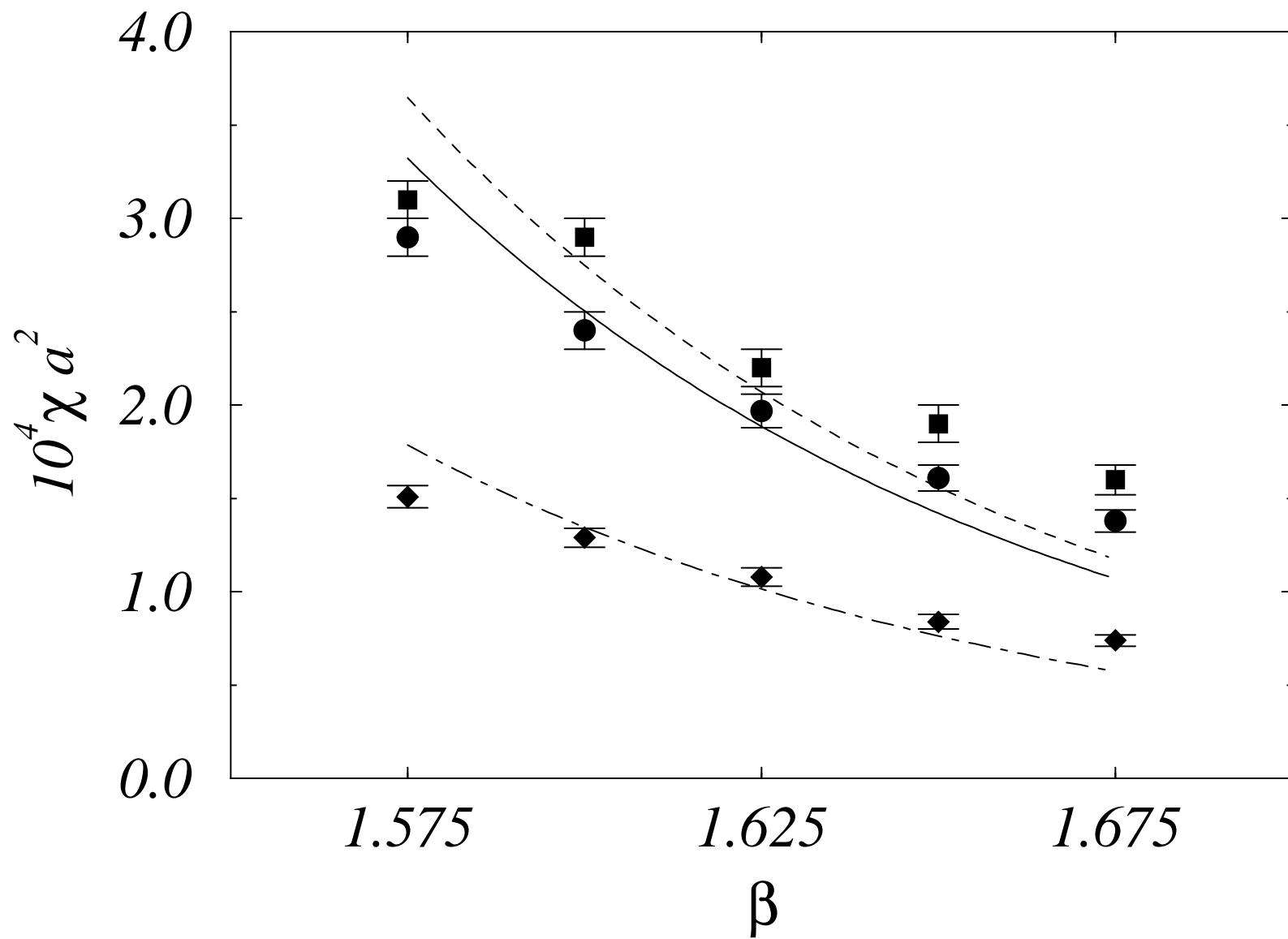


Figure 13

